UC Davis
UC Davis Previously Published Works

Title

Experimental determination of carbonate-associated sulfate δ34S in planktonic foraminifera shells

Permalink

https://escholarship.org/uc/item/6tr2x4v7

Journal

Geochemistry Geophysics Geosystems, 15(4)

ISSN

1525-2027

Authors

Paris, Guillaume
Fehrenbacher, Jennifer S
Sessions, Alex L
et al.

Publication Date

2014-04-01

DOI

10.1002/2014gc005295

Peer reviewed

Experimental determination of carbonate-associated sulfate δ^{34}S in planktonic foraminifera shells

Guillaume Paris[1], Jennifer S. Fehrenbacher[2], Alex L. Sessions[1], Howard J. Spero[2], and Jess F. Adkins[1]

[1]Division of Geological and Planetary Sciences, California Institute of Technology, Pasadena, California, USA, [2]Department of Earth and Planetary Sciences, University of California Davis, Davis, California, USA

Abstract Understanding the coupling of oxygen, carbon, and sulfur cycles in the past is critical for reconstructing the history of biogeochemical cycles, paleoclimatic variations, and oceanic chemistry. The abundance of sulfur isotopes (δ^{34}S) in sulfate from ancient marine carbonates, or carbonate-associated sulfate (CAS), is commonly used, along with other archives (mainly evaporites and barite), to estimate the δ^{34}S of seawater throughout Earth history. Analyses of CAS from hand-picked foraminifera are potentially valuable because this group of organisms is used in numerous paleoceanographic studies. They could provide coupled, high-resolution records of δ^{13}C, δ^{18}O, and δ^{34}S isotopic changes directly linked to orbitally tuned records of climate change through the Cenozoic. Such measurements have not previously been possible due to limitations of sensitivity in conventional IRMS-based techniques. However, the recent development of CAS analysis by multicollector inductively coupled plasma mass spectrometry (MC-ICP-MS) now allows us to work on samples containing just a few nmol of sulfur with accuracy for δ^{34}S values approaching 0.1‰ and, consequently, to analyze hand-picked samples of foraminifera shells. Here we report the results of culture experiments with the planktonic species *Orbulina universa*, that establish a shell:seawater δ^{34}S calibration for future applications to the fossil record. Our new method uses <650 μg of carbonate ($\sim$15 shells) per analysis. The results show that S isotopes are fractionated consistently by -1‰ between seawater and *O. universa* tests. We also demonstrate that *O. universa* faithfully records the [SO$_4^{2-}$]/[Ca^{2+}] ratio of the seawater in which it grew.

1. Introduction

Sulfate (SO$_4^{2-}$) is the second most abundant anion ($\sim$28 mmol L^{-1}) in the modern ocean. It plays a major role in anoxic sediments where microbial sulfate reduction (MSR) is globally the most important anaerobic pathway for organic matter remineralization [*Canfield and Raiswell*, 1999; *Jørgensen*, 1982]. When coupled to pyrite formation, MSR is one of the main sinks of oceanic sulfate. The second sink of marine sulfate is the precipitation of evaporite, mostly from gypsum (CaSO$_4$(2H$_2$O)) and anhydrite (CaSO$_4$), whereas riverine inputs of sulfate to the marine system come from pyrite oxidation or gypsum dissolution on land. The high seawater sulfate concentration reflects its very long residence time of $\sim$20 Ma [*Bottrell and Newton*, 2006; *Newton and Bottrell*, 2007]. As a consequence, the sulfur isotopic composition of the modern ocean is homogeneous (δ^{34}S$_{sw} \approx 21$‰) [*Paris et al.*, 2013; *Rees et al.*, 1978], where

$$\delta^{34}\text{S} = \left[\left(^{34}\text{R}_{sample}/^{34}\text{R}_{VCDT}\right) - 1\right] \tag{1}$$

with

$$^{34}\text{R} = {}^{34}\text{S}/^{32}\text{S} \tag{2}$$

and VCDT (Vienna Canyon Diablo Troilite) is the reference standard [*Coplen and Krouse*, 1998]. In the ocean, microbial sulfate reduction, when combined with pyrite burial, couples the carbon, sulfur, and oxygen cycles. On land, weathering of pyrite consumes atmospheric O$_2$, connecting the oxygen and sulfur cycles. This process generates sulfuric acid which then competes with CO$_2$ for the dissolution of carbonates [*Beaulieu et al.*, 2011; *Calmels et al.*, 2007], thereby linking the terrestrial carbon and sulfur cycles. Quantifying
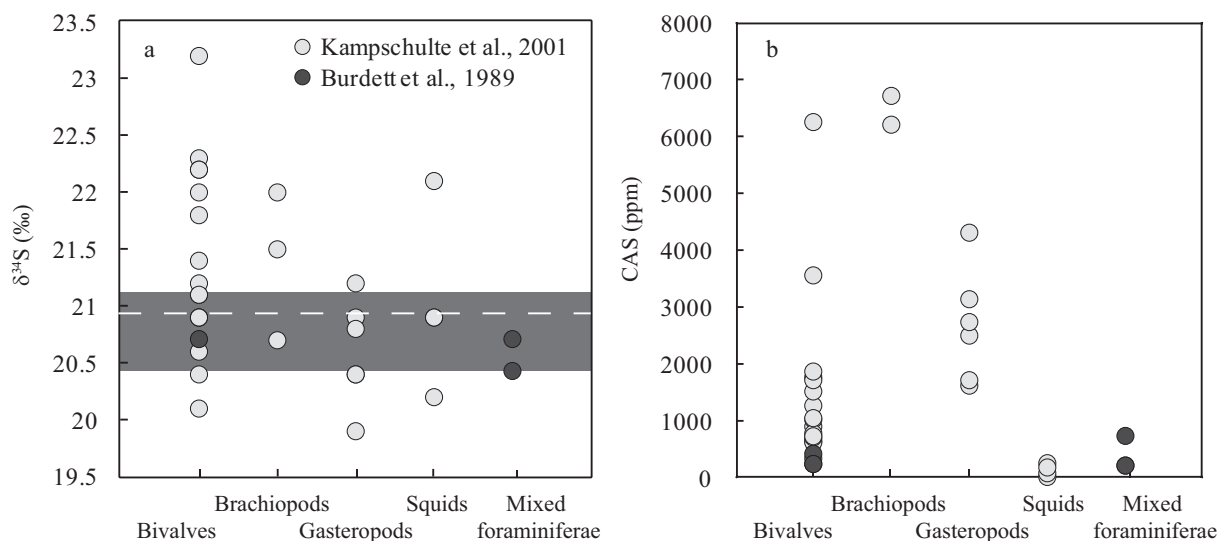
Figure 1. Summary of sulfur isotopic compositions and sulfate contents of CAS from various calcifying organisms. The gray bar in Figure 1a encompasses the mean and 1σ for seawater isotopic composition from *Kampschulte et al.* [2001]. The dashed white line is the mean value from *Paris et al.* [2013].

variations of $\delta^{34}S_{sw}$ though time can help us to understand shifts in the sulfur cycle and constrain its links with the carbon and oxygen cycles.

Early studies measuring carbon and oxygen isotopes in marine carbonates [*Emiliani*, 1955; *Epstein et al.*, 1951; *McKinney et al.*, 1950; *Shackleton*, 1967] provided the paleoceanographic foundation for Cenozoic and Mesozoic reconstructions of Earth's climate and the chemistry of the ocean over the past 250 Ma [*Veizer et al.*, 1999; *Zachos et al.*, 2001]. The need for a comparable sulfur isotope record that could be linked directly to these carbon and oxygen isotope reconstructions has been recognized for many decades [*Garrels and Lerman*, 1981], and a number of studies have pursued this objective using sedimentary archives such as gypsum [*Claypool et al.*, 1980], carbonate-associated sulfate (CAS) [*Burdett et al.*, 1989; *Kah et al.*, 2001; *Kampschulte et al.*, 2001; *Strauss*, 1999], and barite [*Paytan et al.*, 1998, 2004].

The earliest records of marine $\delta^{34}S$ were based on gypsum, in which the isotopic composition of sulfur reflects that of the brine from which it precipitated, with a minor fractionation of sulfur isotopes (hereafter referred to simply as fractionation) [*Claypool et al.*, 1980]. Two inherent characteristics of the evaporite record limit the usefulness of this archive. First, the isotopic composition of the brine may evolve and depart from that of seawater, altering the $\delta^{34}S$ values of sulfate. Second, marine evaporites are temporally discrete by nature, limiting the resolution than can be achieved. The isotopic composition of sulfur from sedimentary barite ($BaSO_4$) has also been used to reconstruct the isotopic composition of seawater [*Paytan et al.*, 1998, 2004]. Barite is insoluble in seawater and is thus assumed to be very resistant to diagenetic changes. As a result, it has become the favored archive for paleoenvironmental reconstruction. Unlike gypsum, fractionation in barite is thought to be minimal and marine barite records from deep sea cores are continuous. However, barite precipitates in specific microenvironments enriched in barium and the potential for isotopic offsets from seawater sulfate have not been fully explored. Moreover, the S-isotopic composition of barite cannot be directly linked to the carbon and oxygen isotopic compositions of seawater and must instead rely on the assumption that barite and carbonate minerals found in the same sediments record the same environments.

Existing measurements of $\delta^{34}S_{CAS}$ on modern marine biogenic carbonates collected from different environments (coastal, benthic, and open ocean) are scattered around the open ocean $\delta^{34}S$ value (Figure 1) [*Burdett et al.*, 1989; *Kampschulte et al.*, 2001]. Following early work on the Neogene [*Burdett et al.*, 1989], sulfur isotope analyses of CAS became more widespread and are now used to investigate the entire Phanerozoic and the Precambrian [e.g., *Fike and Grotzinger*, 2008; *Gill et al.*, 2007; *Kah et al.*, 2001; *Kampschulte et al.*, 2001; *Strauss*, 1999]. However, the form CAS takes in the mineral lattice (e.g., inorganic or organic) has not

Table 1. Composition of the Artificial Seawater (Total Volume of 10 L) Used for Mixing With the Natural Seawater

Salt	Gram	Millimole Per Liter
NaCl	223.3	382.3
$CaCl_2 \cdot 2H_2O$	15.4	10.5
KBr	1	0.8
NaF	0.03	0.1
KCl	7	9.4
H_3BO_3	0.3	0.5
Na_2SO_4	12.2	8.6
$NaHCO_3$	1.6	1.9
$SrCl_2 \cdot 6H_2O$	0.17	0.1
$MgCl_2 \cdot 6H_2O$	111	54.6

yet been resolved [*Cuif et al.*, 2003; *Dauphin et al.*, 2005, 2003; *Erez*, 2003]. Despite these unknowns, CAS is a potentially important archive for sulfur isotopic reconstructions because carbonate microfossils are ubiquitous and readily available to produce continuous records. In particular, foraminifera would have several advantages over barite for a Cenozoic δ^{34}S reconstruction. The depth habitats of many species are well constrained, foraminifera shells are the phase from which most age models are developed, and δ^{34}S data could be directly linked to foraminifera δ^{13}C and δ^{18}O records. However, before such records can be established, the sulfur isotopic relationship between seawater sulfate and $CaCO_3$ produced by foraminifera needs to be quantified.

In this study, we present results from a series of experiments with the planktonic foraminifera *Orbulina universa*, to quantify the relationship between the δ^{34}S of seawater SO_4^{2-} and lattice-bound sulfur in the foraminifera shell. *Orbulina universa* was used because its behavior and life cycle are well known, the environmental and physiological parameters affecting shell geochemistry are well characterized, and it is a robust species in the laboratory [*Bemis et al.*, 2000; *Hönisch et al.*, 2003; *Sanyal et al.*, 1996; *Spero*, 1988, 1992; *Spero et al.*, 1997; *Vetter et al.*, 2013]. Here we present data from foraminiferal calcite obtained by MC-ICP-MS that yield accurate and precise δ^{34}S values for as few as 10–15 *O. universa* shells. As part of this study, we also used nanoscale secondary ion mass spectrometry (NanoSIMS) to quantify the location of the lattice-bound sulfur in a cultured *O. universa* test.

2. Methods

2.1. Culture Experiment

Trochospiral shell, presphere *O. universa* were hand-collected by scuba divers in the Southern California Bight in July 2011 and cultured at the Wrigley Marine Science Center, Santa Catalina Island, California. To control the δ^{34}S and $[SO_4^{2-}]$ of culture waters, we prepared mixtures of ambient seawater and artificial seawater. Ambient seawater was collected 2 km offshore for use in culture experiments and filtered through 0.8 μm nitrate cellulose filters. Ambient seawater had an average pH 7.96 (total scale, offset from the NBS by ∼0.13 pH units) and alkalinity = 2209 μmol kg^{-1}. We prepared synthetic seawater by adding salts to 18.2 MΩ ultrapure MilliQ water to match the concentrations of major cations and anions in seawater, except sulfate (Table 1) [*Morel et al.*, 1979]. The δ^{34}S of sulfate differs by >22‰ in artificial and natural seawaters (−1.82‰ and 20.86‰, respectively), so these waters could be mixed in different proportions (Table 2) to obtain experimental seawaters with different δ^{34}S and $[SO_4^{2-}]$ Each experiment consisted of 15 foraminifera that were cultured independently in aliquots of the same batch of experimental seawater. Following collection, individuals were transferred into 120 mL borosilicate glass jars filled with one of the seawater mixtures, and placed in a water bath maintained at 22.6°C (±0.3°C). Following previously established culturing methods [*Bemis et al.*, 1998; *Lea et al.*, 1999], each specimen was maintained in individual jars under high light (>350 μmol photons m^{-2} s^{-1}) and fed a 1 day old *Artemia nauplius* every other day. After several days in culture, *O. universa* secretes a spherical chamber that continues to thicken until gametogenesis [*Spero*,

Table 2. Chemical and Isotopic Composition of the Four Experimental Seawaters Used in This Study[a]

	Alk	pH	f	$\delta^{34}S_{VCDT}$	1σ	$[SO_4^{2-}]^1$	SO_4^{2-}/Ca^{2+b}
Experiment 1	2273	8.22	0.5	14.18‰	0.10	18.3	4.03
Experiment 2	2264	8.02	0.33	16.88‰	0.13	20.8	4.56
Experiment 3	2243	8.00	0.17	19.04‰	0.06	24.1	5.19
Experiment 4	2204	7.90	0	20.86‰	0.11	27.9	5.96

[a]Alk = alkalinity (μg/g); f = artificial seawater/(natural seawater + artificial seawater); 1 = concentrations in mmol L^{-1}, measured at 5% 1σ.
[b]Ratios in g/g, measured at 2.5% 1σ.

1988], after which the empty tests were collected, rinsed in MilliQ water, and archived in 10 hole micropaleoslides for later analysis.

2.2. Isotopic Composition

All spherical tests obtained from an experimental group were pooled, cracked-open, soaked for 30 min in a 50:50 solution of 30% H_2O_2 and 0.1M NaOH at 60°C to remove remnant organic matter, and rinsed three times in MilliQ water. Samples were dissolved using ultrapure Baseline Seastar HCl and dried down on a hot plate in a PicoTrace (trace metal clean) hood at 110°C. Following the procedure of *Paris et al.* [2013], the residues were dissolved in 40 μL of 0.25% Seastar HCl and eluted through a column containing 20 μL of precleaned AG50X8 cationic exchange resin to remove cations. The resin was rinsed with 3×20 μL of 0.25% Seastar HCl to ensure complete recovery of sulfate.

Following purification, sulfur isotopes were analyzed on the ThermoScientific Neptune Plus MC-ICP-MS using a desolvating membrane (Aridus, Cetac) to minimize O_2 isobaric interference, and with sample-standard bracketing to correct for instrumental mass fractionation drift [*Paris et al.*, 2013]. The bracketing standard solution contained 5 μM sulfate and the samples were adjusted to reach sulfate concentrations at or below this level. All isotope ratios were corrected for instrumental fractionation, by assuming linear drift between successive standards, and for instrumental background. Concentrations were measured on a DX500 Dionex Ion Chromatograph.

2.3. Data Processing

Measured sulfate concentrations and isotope ratios were corrected for procedural blanks by mass balance. The amount of sulfate in the foraminifera samples is given by

$$n_{foram} = n_{meas} - n_{blank} \tag{3}$$

where n represents the number of moles of sulfate in a *foraminifera* sample, in the total *measured* sample, or in the procedural *blank*. The concentration of sulfate (in ppm) is then calculated as

$$\left[SO_4{}^{2-}\right]_{foram} = (n_{foram} \times 96.04)/m_{carb} \tag{4}$$

where m_{carb} is the total mass of carbonate collected for each experiment. Similarly, the blank-corrected isotopic composition is given by

$$\delta^{34}S_{foram} = [(\delta^{34}S_{meas} \times n_{meas}) - (\delta^{34}S_{blank} \times n_{blank})]/n_{foram}. \tag{5}$$

We measured $n_{blank} = 0.13 \pm 0.06$ nmol (1sd, n = 3) with a $\delta^{34}S_{blank}$ value of $-2.21 \pm 0.4‰$ (1sd, n = 3).

Because the foraminifera were collected as juveniles from the ocean, 5–10% of the shell calcite (trochospiral shell) was precipitated under marine, rather than experimental, conditions [*Spero and Parker*, 1985]. We assume that this juvenile calcite has the same sulfate abundance (n_{foram}) and isotopic composition ($\delta^{34}S_{foram}$) as the foraminifera from Experiment 4 grown in ambient seawater. We correct for this nonexperimental shell material using the same mass balance equations described above for the procedural blank. Uncertainty in the corrected $\delta^{34}S$ and concentration values is calculated by a Monte Carlo method, propagating the standard deviation obtained for random populations of 1000 values with a normal distribution characterized by the standard deviation estimated for each member of equations (4) and (5).

2.4. NanoSIMS

Ion probe analyses were performed on the Cameca NanoSIMS 50-L at Caltech. Mg and Ca are usually analyzed using a $^{16}O^-$ primary beam to form positive ions. However, S and O are best measured as negative ions ($^{32}S^-$ and $^{18}O^-$) using a Cs^+ primary beam. In order to measure Mg, Ca, S, and O simultaneously, all elements were collected using a $^{133}Cs^+$ primary beam ($\sim$1 pA) and Mg and Ca were measured as their oxide anions ($^{24}Mg^{16}O^-$ and $^{40}Ca^{16}O^-$, respectively). Results are shown as ratios of MgO/CaO and S/O. We normalized monoatomic and oxide ions against each other to account more accurately for instrumental mass bias. Data were collected from a fragment of the shell of an individual *O. universa* designated "EN1"

Table 3. Sulfate Content and Isotopic Composition for the Foraminifera Analyzed in This Study

	Drift Corrected $\delta^{34}S_{VCDT}$a (‰)	TPB Corrected $\delta^{34}S_{VCDT}$ (‰)	1σ	Juvenile Calcite Corrected $\delta^{34}S_{VCDT}$ (‰)	1σ	SO_4^{2-}/Ca^{2+} ($\mu g/g$)	1σ	Calcite (mg)	1σ
Exp. 1	13.89	14.15	0.24	13.42	0.39	1062	63	0.632	15
Exp. 2	15.39	15.77	0.29	15.29	0.35	1164	68	0.420	13
Exp. 3	17.96	18.27	0.25	18.09	0.29	1289	74	0.547	15
Exp. 4	19.45	19.95	0.33	19.95	0.33	1651	892	0.294	13

aThe analytical reproducibility of the samples is evaluated based on the coral *Desmophyllum diantus* (0.20‰ 1σ, n = 9). See section 4.

which was maintained in ambient seawater at 18°C with a 12:12 reversed light/dark schedule (i.e., light from 7 pm to 7 am). This specimen was part of a different experiment series, and the reverse light cycle should have no effect on shell sulfur. The shell was embedded under vacuum in EpoFix epoxy at UC Davis. It was then successively ground and polished using a series of diamond grinding disks, 3 μm WCA alumina/water slurry on glass, Buehler 1.0 μm alumina Micropolish on a Buehler Texmet pad, then Buehler 0.3 μm alumina Micropolish on a Microcloth pad. The sample was then carbon coated and analyzed. A succession of 40 rasters of an 18 by 18 μm area (256 by 256 pixels) was collected, each acquisition lasting 15 min for a total of 10 h.

3. Results

3.1. Isotopic Compositions

Concentrations and isotopic compositions of the culture water and foraminifera from each experiment are reported in Tables 2 and 3 and plotted in Figure 2. The $\delta^{34}S$ values of *O. universa* CAS are highly correlated with those of sulfate in the culture water. A regression performed using Isoplot (K.R. Ludwig, Berkeley Geochronology Center) based on the algorithm of *York* [1968], which accounts for differing uncertainties in both variables for each data point, yields a regression line defined according to equation (6)

$$\delta^{34}S_{foram} = 1.012 \ (\pm 0.015) \times \delta^{34}S_{sw} - 1.3 \ (\pm 2.7) \tag{6}$$

with a MSDW of 1.3, suggesting that analytical errors explain the observed scatter around the trend (Table 4). The fractionation between seawater and *O. universa* ($\varepsilon_{foram/sw}$) is calculated as

$$\varepsilon_{foram/sw} = \left(\left(\delta^{34}S_{foram} + 1 \right) / \left(\delta^{34}S_{sw} + 1 \right) - 1 \right). \tag{7}$$

The average fractionation for the four experiments is -1.03 ± 0.70‰ (2σ, n = 4).

3.2. Sulfur Content and Distribution in the Shell

Bulk sulfate concentrations in shells and culture seawater are conveniently compared using the distribution coefficient

$$K_d = \frac{[SO_4^{2-}]/[Ca^{2+}]_{orbulina}}{[SO_4^{2-}]/[Ca^{2+}]_{sw}} \tag{8}$$

The average K_d is $261 \pm 11 \times 10^{-6}$ (Table 5) and, similar to the isotopic fractionation, shows no significant variation between experiments.

Micron-scale spatial variability of sulfur incorporation in the foraminifera shell is clearly visible in the NanoSIMS rasters and profiles (Figure 3). Both Mg/Ca and S/O ratios are characterized by strong banding following the growth layers (Figure 3). The position of the banding is similar, but not identical, for the two elements and appears to be more subparallel to the sides of the shell walls for Mg/Ca than for S/O (Figure 3c). For instance, profile 2 is located along the highest S/O values and the correspondence between Mg/Ca and S/O peaks is less strict than on profiles 1 and 3. In this area, the S/O bands are not as subparallel to the foraminifera walls as the Mg/Ca bands are.
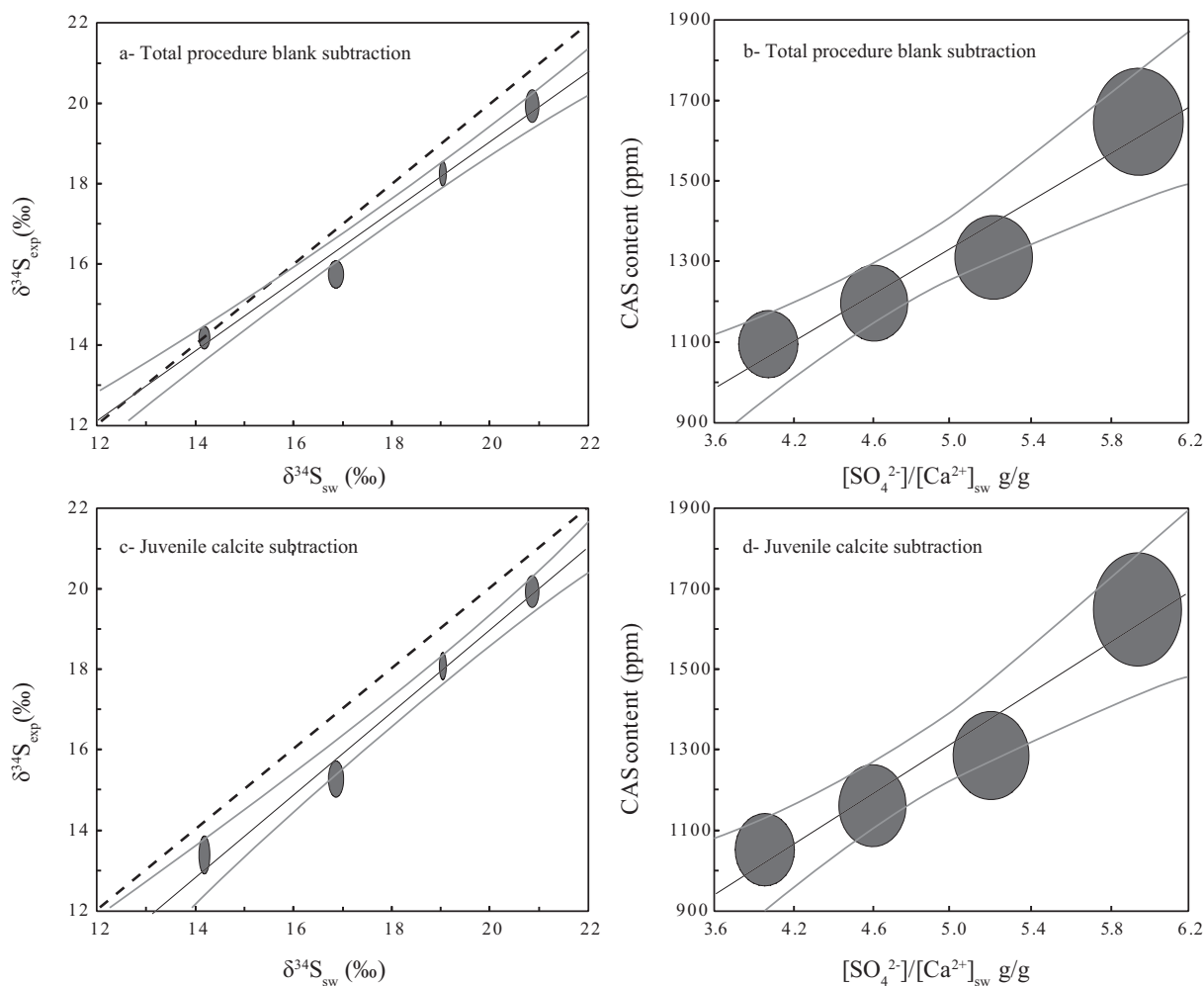
Figure 2. Comparison of sulfur isotopic compositions and sulfate contents of *Orbulina universa* CAS versus culture water. Plotted values in Figures 1a and 1b are corrected for the procedural blank, and those in Figures 1c and 1d are also corrected for trochospiral shell calcite. Error ellipses are given as 1σ.

4. Discussion

Our data show that *O. universa* shells faithfully record both the sulfate $\delta^{34}S$ value and the SO_4^{2-}/Ca^{2+} ratio of seawater, with systematic offsets. The isotopic fractionation by this species is constant over the range of seawater chemistries studied, although CAS data from other calcifying organisms suggest much greater variance [*Burdett et al.*, 1989; *Kampschulte and Strauss*, 2004]. In an attempt to confirm that this variance in the offset is biological rather than analytical in origin, we measured the sulfur isotopic composition of one specimen of the deep-sea coral *Desmophyllum diantus* collected off Tasmania during the Southern Surveyor cruise (SS0108 STA011 13 January 2008). Sulfur isotopes from this coral ($\delta^{34}S = 22.18 \pm 0.39‰$, 2σ, n = 9; three independent purifications of powder from one individual, measured three times each), are fractionated by ca. $+1.3‰$ compared to seawater and the K_d value is 880×10^{-6} (assuming mean oceanic $[SO_4^{2-}]$ and $[Ca^{2+}]$ of 28.2 and 10.3 mmol L^{-1}, respectively). These

Table 4. Slope, Intercept, and MSWD (Mean Square Weighted Deviation) of the Regressions Between Seawater Sulfate and CAS Isotopic Composition and Concentrations Calculated Using Isoplot Based on a York Regression[a]

	Regression Parameters	TPB Corrected	Juvenile Calcite Corrected
$\delta^{34}S_{VCDT}$	Slope	0.873 ± 0.11	1.012 ± 0.15
	Intercept	1.57 ± 2	−1.2 ± 2.7
	MSWD	2	1.3
Concentrations	Slope	265 ± 110	287 ± 120
	Intercept	−10 ± 510	−127 ± 560
	MSWD	0.78	0.75

[a]Errors are given as 2σ.

Table 5. Fractionation Factor ε (‰) and Distribution Coefficients K_d for Each Individual Experiment and Average Values

Experiment	ε	K_d
Exp. 1	−0.76	264×10^{-6}
Exp. 2	−1.55	255×10^{-6}
Exp. 3	−0.93	248×10^{-6}
Exp. 4	−0.89	277×10^{-6}
Average	−1.03	261×10^{-6}
Std. dev.[a]	0.35	11×10^{-6}

[a]Standard deviation.

data confirm that there are differences in sulfate incorporation and isotopic offsets from seawater among different marine phyla during skeletal calcification. Whether such large differences exist between foraminifera species remains an open question.

Variability in the isotopic fractionation of sulfur in marine calcifiers could be related to the inorganic processes controlling SO_4 incorporation into calcite. Unfortunately, little is known about the location and mechanism of sulfate incorporation into the calcium carbonate lattice [*Staudt et al.*, 1994]. In all calcifiers, sulfate must be excluded from the precipitating crystal because there is more sulfate in seawater than both calcium and carbonate ion. Compared to the planar carbonate ion, the sulfate group is bigger and tetrahedral. However, calcite precipitation experiments suggest sulfate is substituted for the carbonate ion as calcite grows. It is interpreted to be preferentially included in kink sites where the three neighbor calcium atoms are located in the same atomic layer, making this a less constrained and bigger site, thus more likely to accept sulfate [*Staudt et al.*, 1994]. An overall positive correlation has been observed between the distribution coefficient and the growth rate during synthetic calcite precipitation experiments [*Busenberg and Plummer*, 1985], but the exact mechanisms of incorporation remain elusive. These inorganic processes are likely to drive $\delta^{34}S$ in one direction relative to an inorganic reference frame and might therefore be an unlikely candidate to explain marine calcifiers that are both heavier and lighter than seawater. However, we do not yet have good experimental data on the $\delta^{34}S$ of CAS precipitated at equilibrium. Lab experiments of this type are clearly an important next step.

In addition to inorganic sulfate, biogenic carbonates can contain organic matrix sulfur in components such as glycosaminoglycans [*Bé and Ericson*, 1963] or the amino acids, methionine and cysteine. For corals and mollusks, sulfate has been proposed to be primarily located in the organic matrix using both X-ray
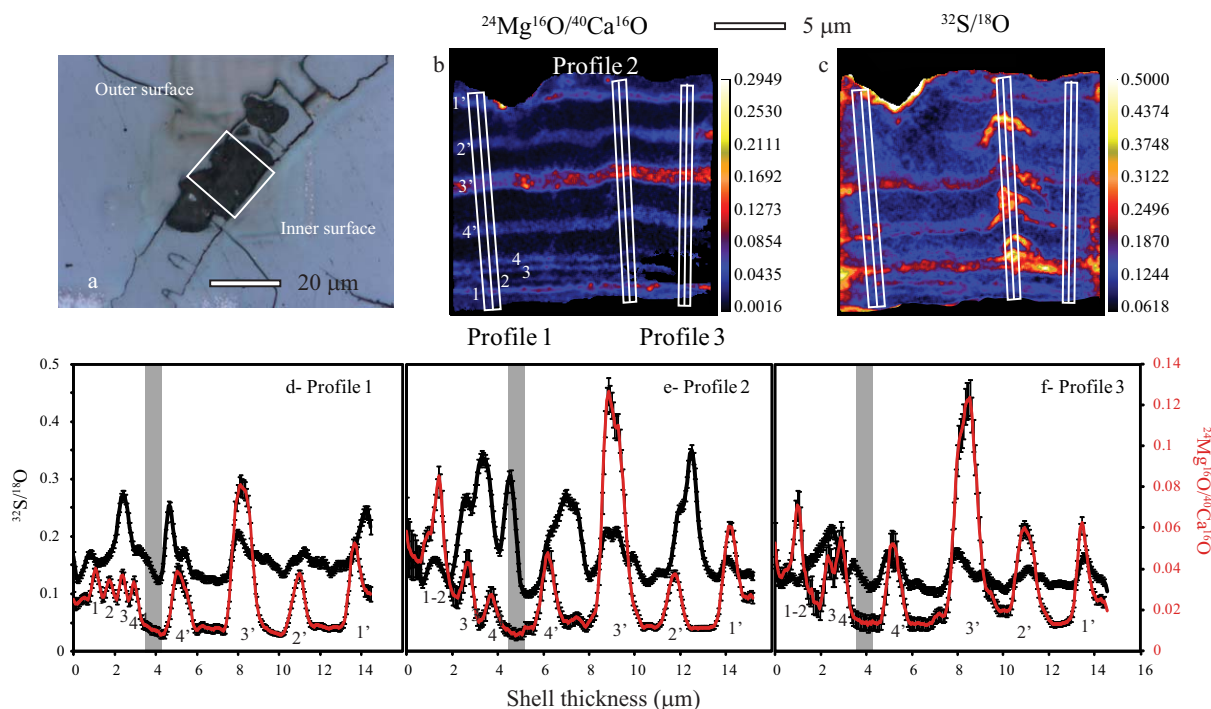

Figure 3. Elemental distributions in a foram shell. (a) Microphotograph of *Orbulina universa* shell embedded in epoxy. (b) MgO/CaO map. (c) S/O map. (c–e) Profiles for both MgO/CaO (gray) and S/O (black) across the shell fragment. The gray bars indicate location of the POM. Data in Figures 1b–1f were obtained from the NanoSIMS raster images and represent the summation of rasters 2–40 (raster 1 was discarded due to an offset in position).

absorption near-edge structure spectroscopy (XANES) at the K-edge of sulfur and Raman spectroscopy [*Cuif et al.*, 2003; *Dauphin et al.*, 2005, 2003]. These authors identified S associated with both amino acids and sulfated polysaccharides (chondroitin sulfate), the latter promoting the precipitation and orientation of calcium carbonates [*Addadi et al.*, 1987]. However, sulfur in amino acids is fully reduced and covalently bonded to the carbon backbone (as thiol functional groups), and so would have to be fully oxidized prior to the ion exchange purification of sulfate. In the case of foraminifera, these molecules are concentrated in the organic matrix, and more precisely for *O. universa* within the primary organic membrane (POM) [*Bé et al.*, 1979; *Spero*, 1988]. This organic layer is the biomineralizing matrix that coincides with initial calcification of the spherical shell. Mg/Ca banding has been reported on both the inside and outside of the *O. universa* sphere [*Eggins et al.*, 2004], although the POM itself is Mg-poor [*Sadekov et al.*, 2005].

The departure of biogenic calcite or aragonite δ^{34}S from that of seawater could potentially be explained either by a mixture of these three organic sources of sulfur or by still-to-be-determined inorganic fractionation. Hypothetically, if we assume that CAS is not fractionated versus seawater, the departure of the isotopic composition could be explained by a mixed contribution of sulfur from CAS and organic sulfur. However, cleaning tests on mollusks designed to remove organic matter show no variation of the sulfur isotopic composition even though the measured concentration of sulfate is reduced, leading to the conclusion that any sulfur carried by the organic phase has an isotopic composition that is the same as inorganic sulfate [*Burdett et al.*, 1989]. If this is true for foraminifera as well, our data cannot be explained by mixing between organic and inorganic sulfur. Furthermore, mass balance dictates that the sulfur we measured as CAS must be overwhelmingly inorganic. The CAS content of *Orbulina* can be as high as ∼1650 ppm (or 0.16 wt % of the shell), which corresponds to ∼0.05 wt % sulfur. Oxidative cleaning removes the leftover protoplasm from the shell, but it may not be able to remove the organic matrix intimately associated with CaCO$_3$. Assuming the organic matrix represents 0.2% of the shell weight [*Weiner and Erez*, 1984], this would require 75% of the mass of the organic matrix to be sulfate to explain all of the sulfur we find in the shell, which is clearly unrealistic. Most of the sulfur in the organic matrix probably resides in amino acids that are likely to bear an isotopic composition significantly different from seawater. Proteins account for about 10% of the matrix [*Nürnberg et al.*, 1996; *Weiner and Erez*, 1984], ∼13 wt % of which on average are methionine, with no numbers reported for cysteine [*Robbins and Brew*, 1990]. These numbers imply that ∼1.1% of the total sulfur in the shell is organic, which would require the δ^{34}S of this pool to be ∼−70‰ to explain the ∼−1‰ offset from seawater measured in Experiment 4. This calculation is sensitive to the ratio of methionine to cysteine because of the substantially different molecular weights for these two molecules. For the assimilitory pathways in these marine calcifiers, a very negative δ^{34}S value for the protenacious sulfur seems unlikely.

Finally, it is unlikely the sulfur isotopic composition of cysteine and methionine could be reset in only a few days as most of the organic precursors for these amino acids likely come from the *Artemia nauplii* the foraminifera are being fed. In contrast, because of a constant fractionation and K$_d$, our data strongly suggest the inorganic incorporation of sulfate into the shell is the dominant source of measured CAS. This interpretation is further supported by NanoSIMS data. NanoSIMS elemental maps show a very specific distribution of sulfur, with banding similar to the well-documented Mg/Ca banding [*Eggins et al.*, 2004]. Minor differences between the two patterns arise from a lower peak height to background ratio for S/O, suggesting an overall more homogeneous distribution for sulfur than for magnesium, and also from the less straight shape of the S/O bands (Figure 3c). These data show that sulfur is not associated with the organic rich POM which is found between the low-Mg band separating the four broadly spaced Mg-rich bands on the outside and the four closely spaced Mg-rich bands on the inner side of the shell (Figure 3). These images also suggest that the behavior of S is coupled to the banding behavior of Mg, in agreement with observations performed on *Amphistegina lobifera* [*Erez*, 2003]. Even if the ultimate control for Mg/Ca dark/light banding remains debated, it does not reflect variations in organic matter content [*Sadekov et al.*, 2005]. Based on these observations, we conclude that our NanoSIMS data support the idea that nearly all of the sulfur in *Orbulina universa* is present as inorganic CAS. Hence, the isotopic fractionation must be associated with inorganic processes, even though equilibrium fractionation and kinetic effects during the incorporation of sulfate within carbonates are not known.

As previously mentioned, we also noticed that the CAS content of the cultured *O. universa* depends on the seawater sulfate concentration. However, the sulfate content of our cultured *Orbulina* is higher than CAS content (∼700 ppm) measured in Atlantic core-top specimens [*Berry*, 1998]. Such an observation could be

due to early diagenesis of the tests on the seafloor. Alternatively, differences in K_d could be due to the existence of distinct genotypes of *Orbulina* in the Caribbean and the Southern California Bright [*Darling et al.*, 1999]. Further work is required to understand the evolution and preservation of sulfur distribution and concentration in the test as it sinks through the water column (live specimens, plankton tows, sediments traps, and core-tops) and/or the difference between clusters of *Orbulina universa* genotypes. We would then be able to offer a new proxy for seawater sulfate concentration.

5. Conclusions

Using MC-ICP-MS, we are able to measure the sulfur-isotopic composition of CAS in samples containing <0.65 mg of carbonate and thus to accurately and precisely measure only 10–15 foraminifera shells. Growth cultures of *O. universa*, in which the concentration and δ^{34}S of growth water sulfate was systematically manipulated, demonstrate that there is a constant S isotope fractionation between sulfate in *O. universa* shells and the seawater in which they grew ($\varepsilon = -1.03 \pm 0.35\permil$; 1sd, n = 4). There is also a constant partitioning of sulfate over the range of studied concentrations ($K_d = 261 \pm 11 \times 10^{-6}$; 1sd, n = 4). Provided there are not confounding diagenetic reactions that change the SO_4^{2-}/Ca^{2+} ratio, *O. universa* CAS could be a good proxy for seawater sulfate in oceanic sediment cores, and would provide a direct route to coeval records of δ^{13}C, δ^{18}O, δ^{34}S, and $[SO_4^{2-}]$ of the oceans through geologic times.

References

Addadi, L., J. Moradian, E. Shay, N. G. Maroudas, and S. Weiner (1987), A chemical model for the cooperation of sulfates and carboxylates in calcite crystal nucleation: Relevance to biomineralization, *Proc. Natl. Acad. Sci. U.S.A.*, 84(9), 2732–2736.

Bé, A. W. H., and D. B. Ericson (1963), Aspects of calcifications in planktonic foraminifera (Sarcodina), *Ann. N. Y. Acad. Sci.*, 109(1), 65–81, doi: 10.1111/j.1749-6632.1963.tb13462.x.

Bé, A. W. H., C. Hemleben, O. R. Anderson, and M. Spindler (1979), Chamber formation in planktonic foraminifera, *Micropaleontology*, 25(3), 294–307, doi:10.2307/1485304.

Beaulieu, E., Y. Goddéris, D. Labat, C. Roelandt, D. Calmels, and J. Gaillardet (2011), Modeling of water-rock interaction in the Mackenzie basin: Competition between sulfuric and carbonic acids, *Chem. Geol.*, 289(1–2), 114–123, doi:10.1016/j.chemgeo.2011.07.020.

Bemis, B. E., H. J. Spero, J. Bijma, and D. W. Lea (1998), Reevaluation of the oxygen isotopic composition of planktonic foraminifera: Experimental results and revised paleotemperature equations, *Paleoceanography*, 13(2), 150–160, doi:10.1029/98PA00070.

Bemis, B. E., H. J. Spero, D. W. Lea, and J. Bijma (2000), Temperature influence on the carbon isotopic composition of Globigerina bulloides and Orbulina universa (planktonic foraminifera), *Mar. Micropaleontol.*, 38(3–4), 213–228, doi:10.1016/S0377-8398(00)00006-2.

Berry, J. N. (1998), Sulfate in foraminiferal calcium carbonate: Investigating a potential proxy for sea water carbonate ion concentration, MS thesis, 88 p., Mass. Inst. of Technol., Cambridge, Mass.

Bottrell, S. H., and R. J. Newton (2006), Reconstruction of changes in global sulfur cycling from marine sulfate isotopes, *Earth Sci. Rev.*, 75(1–4), 59–83, doi:10.1016/j.earscirev.2005.10.004.

Burdett, J., M. Arthur, and M. Richardson (1989), A Neogene seawater sulfur isotope age curve from calcareous pelagic microfossils, *Earth Planet. Sci. Lett.*, 94, 189–198, doi:10.1016/0012-821X(89)90138-6.

Busenberg, E., and L. N. Plummer (1985), Kinetic and thermodynamic factors controlling the distribution of SO_3^{2-} and Na^+ in calcites and selected aragonites, *Geochim. Cosmochim. Acta*, 49(3), 713–725, doi:10.1016/0016-7037(85)90166-8.

Calmels, D., J. Gaillardet, A. Brenot, and C. France-Lanord (2007), Sustained sulfide oxidation by physical erosion processes in the Mackenzie River basin: Climatic perspectives, *Geology*, 35(11), 1003–1006, doi:10.1130/G24132A.1.

Canfield, D. E., and R. Raiswell (1999), The evolution of the sulfur cycle, *Am. J. Sci.*, 299(7–9), 697–723, doi:10.2475/ajs.299.7-9.697.

Claypool, G., W. Holser, I. Kaplan, H. Sakai, and I. Zak (1980), The age curves of sulfur and oxygen isotopes in marine sulfate and their mutual interpretation, *Chem. Geol.*, 28, 199–260, doi:10.1016/0009-2541(80)90047-9.

Coplen, T. B., and H. R. Krouse (1998), Sulphur isotope data consistency improved, *Nature*, 392(6671), 32–32, doi:10.1038/32080.

Cuif, J.-P., Y. Dauphin, J. Doucet, M. Salome, and J. Susini (2003), XANES mapping of organic sulfate in three scleractinian coral skeletons, *Geochim. Cosmochim. Acta*, 67(1), 75–83, doi:10.1016/S0016-7037(02)01041-4.

Darling, K. F., C. M. Wade, D. Kroon, A. J. L. Brown, and J. Bijma (1999), The diversity and distribution of modern planktic foraminiferal small subunit ribosomal RNA genotypes and their potential as tracers of present and past ocean circulations, *Paleoceanography*, 14(1), 3–12, doi:10.1029/1998PA900002.

Dauphin, Y., J.-P. Cuif, J. Doucet, M. Salomé, J. Susini, and C. Terry Willams (2003), In situ chemical speciation of sulfur in calcitic biominerals and the simple prism concept, *J. Struct. Biol.*, 142(2), 272–280, doi:10.1016/S1047-8477(03)00054-6.

Dauphin, Y., J.-P. Cuif, M. Salomé, and J. Susini (2005), Speciation and distribution of sulfur in a mollusk shell as revealed by in situ maps using X-ray absorption near-edge structure (XANES) spectroscopy at the S K-edge, *Am. Mineral.*, 90(11–12), 1748–1758, doi:10.2138/am.2005.1640.

Eggins, S. M., A. Sadekov, and P. De Deckker (2004), Modulation and daily banding of Mg/Ca in Orbulina universa tests by symbiont photosynthesis and respiration: A complication for seawater thermometry?, *Earth Planet. Sci. Lett.*, 225(3–4), 411–419, doi:10.1016/j.epsl.2004.06.019.

Emiliani, C. (1955), Pleistocene temperatures, *J. Geol.*, 63, 538–578.

Epstein, S., R. Buchsbaum, H. Lowenstam, and H. C. Urey (1951), Carbonate-water isotopic temperature scale, *Geol. Soc. Am. Bull.*, 62(4), 417–426, doi:10.1130/0016-7606(1951)62[417:cits]2.0.co;2.

Erez, J. (2003), The source of ions for biomineralization in foraminifera and their implications for paleoceanographic proxies, *Rev. Mineral. Geochem.*, 54(1), 115–149, doi:10.2113/0540115.

Fike, D. A., and J. P. Grotzinger (2008), A paired sulfate–pyrite δ^{34}S approach to understanding the evolution of the Ediacaran–Cambrian sulfur cycle, *Geochim. Cosmochim. Acta*, *72*(11), 2636–2648, doi:10.1016/j.gca.2008.03.021.

Garrels, R. M., and A. Lerman (1981), Phanerozoic cycles of sedimentary carbon and sulfur, *Proc. Natl. Acad. Sci. U.S.A.*, *78*(8), 4652–4656.

Gill, B. C., T. W. Lyons, and M. R. Saltzman (2007), Parallel, high-resolution carbon and sulfur isotope records of the evolving Paleozoic marine sulfur reservoir, *Palaeogeogr. Palaeoclimatol. Palaeoecol.*, *256*(3–4), 156–173, doi:10.1016/j.palaeo.2007.02.030.

Hönisch, B., J. Bijma, A. D. Russell, H. J. Spero, M. R. Palmer, R. E. Zeebe, and A. Eisenhauer (2003), The influence of symbiont photosynthesis on the boron isotopic composition of foraminifera shells, *Mar. Micropaleontol.*, *49*, 87–96, doi:10.1016/S0377-8398(03)00030-6.

Jørgensen, B. B. (1982), Mineralization of organic matter in the sea bed-the role of sulphate reduction, *Nature*, *296*(5858), 643–645, doi: 10.1038/296643a0.

Kah, L. C., T. W. Lyons, and J. T. Chesley (2001), Geochemistry of a 1.2 Ga carbonate-evaporite succession, northern Baffin and Bylot Islands: Implications for mesoproterozoic marine evolution, *Precambrian Res.*, *111*(1–4), 203–234, doi:10.1016/s0301-9268(01)00161-9.

Kampschulte, A., and H. Strauss (2004), The sulfur isotopic evolution of Phanerozoic seawater based on the analysis of structurally substituted sulfate in carbonates, *Chem. Geol.*, *204*(3–4), 255–286, doi:10.1016/j.chemgeo.2003.11.013.

Kampschulte, A., P. Bruckschen, and H. Strauss (2001), The sulphur isotopic composition of trace sulphates in Carboniferous brachiopods: Implications for coeval seawater, correlation with other geochemical cycles and isotope stratigraphy, *Chem. Geol.*, *175*(1–2), 149–173, doi:10.1016/S0009-2541(00)00367-3.

Lea, D. W., T. A. Mashiotta, and H. J. Spero (1999), Controls on magnesium and strontium uptake in planktonic foraminifera determined by live culturing, *Geochim. Cosmochim. Acta*, *63*(16), 2369–2379, doi:10.1016/S0016-7037(99)00197-0.

McKinney, C., J. McCrea, S. Epstein, H. Allen, and H. Urey (1950), Improvements in mass spectrometers for the measurement of small differences in isotope abundance ratios, *Rev. Sci. Instrum.*, *21*(8), 724–730, doi:10.1063/1.1745698.

Morel, F. M. M., J. G. Rueter, D. M. Anderson, and R. R. L. Guillard (1979), AQUIL: A chemically defined phytoplankton culture medium for trace metal studies, *J. Phycol.*, *15*(2), 135–141, doi:10.1111/j.1529-8817.1979.tb02976.x.

Newton, R., and S. Bottrell (2007), Stable isotopes of carbon and sulphur as indicators of environmental change: Past and present, *J. Geol. Soc.*, *164*(4), 691–708, doi:10.1144/0016-76492006-101.

Nürnberg, D., J. Bijma, and C. Hemleben (1996), Assessing the reliability of magnesium in foraminiferal calcite as a proxy for water mass temperatures, *Geochim. Cosmochim. Acta*, *60*(5), 803–814, doi:10.1016/0016-7037(95)00446-7.

Paris, G., A. L. Sessions, A. V. Subhas, and J. F. Adkins (2013), MC-ICP-MS measurement of δ^{34}S and Δ^{33}S in small amounts of dissolved sulfate, *Chem. Geol.*, *345*, 50–61, doi:10.1016/j.chemgeo.2013.02.022.

Paytan, A., M. Kastner, D. Campbell, and M. H. Thiemens (1998), Sulfur isotopic composition of cenozoic seawater sulfate, *Science*, *282*(5393), 1459–1462, doi:10.1126/science.282.5393.1459.

Paytan, A., M. Kastner, D. Campbell, and M. H. Thiemens (2004), Seawater sulfur isotope fluctuations in the Cretaceous, *Science*, *304*(5677), 1663–1665, doi:10.1126/science.1095258.

Rees, C. E., W. J. Jenkins, and J. Monster (1978), The sulphur isotopic composition of ocean water sulphate, *Geochim. Cosmochim. Acta*, *42*(4), 377–381, doi:10.1016/0016-7037(78)90268-5.

Robbins, L. L., and K. Brew (1990), Proteins from the organic matrix of core-top and fossil planktonic foraminifera, *Geochim. Cosmochim. Acta*, *54*(8), 2285–2292, doi:10.1016/0016-7037(90)90052-M.

Sadekov, A. Y., S. M. Eggins, and P. De Deckker (2005), Characterization of Mg/Ca distributions in planktonic foraminifera species by electron microprobe mapping, *Geochem. Geophys. Geosyst.*, *6*, Q12P06, doi:10.1029/2005GC000973.

Sanyal, A., N. G. Hemming, W. S. Broecker, D. W. Lea, H. J. Spero, and G. N. Hanson (1996), Oceanic pH control on the boron isotopic composition of foraminifera: Evidence from culture experiments, *Paleoceanography*, *11*(5), 513–518, doi:10.1029/96PA01858.

Shackleton, N. (1967), Oxygen isotope analyses and pleistocene temperatures re-assessed, *Nature*, *215*(5096), 15–17, doi:10.1038/215015a0.

Spero, H. J. (1988), Ultrastructural examination of chamber morphogenesis and biomineralization in the planktonic foraminifer *Orbulina universa*, *Mar. Biol.*, *99*(1), 9–20, doi:10.1007/bf00644972.

Spero, H. J. (1992), Do planktic foraminifera accurately record shifts in the carbon isotopic composition of seawater ΣCO_2?, *Mar. Micropaleontol.*, *19*(4), 275–285, doi:10.1016/0377-8398(92)90033-G.

Spero, H. J., and S. L. Parker (1985), Photosynthesis in the symbiotic planktonic foraminifer Orbulina universa, and its potential contribution to oceanic primary productivity, *J. Foraminifer. Res.*, *15*(4), 273–281, doi: 10.2113/gsjfr.15.4.273.

Spero, H. J., J. Bijma, D. W. Lea, and B. E. Bemis (1997), Effect of seawater carbonate concentration on foraminiferal carbon and oxygen isotopes, *Nature*, *390*, 497–500, doi:10.1038/37333.

Staudt, W. J., R. J. Reeder, and M. A. A. Schoonen (1994), Surface structural controls on compositional zoning of SO_4^{2-} and SeO_4^{2-} in synthetic calcite single crystals, *Geochim. Cosmochim. Acta*, *58*(9), 2087–2098, doi:10.1016/0016-7037(94)90287-9.

Strauss, H. (1999), Geological evolution from isotope proxy signals––Sulfur, *Chem. Geol.*, *161*(1–3), 89–101, doi:10.1016/S0009-2541(99)00082-0.

Veizer, J., D. Ala, K. Azmy, P. Bruckschen, D. Buhl, F. Bruhn, G. A. F. Carden, A. Diener, S. Ebneth, and Y. Godderis (1999), ^{87}Sr/^{86}Sr, δ^{13}C and δ^{18}O evolution of Phanerozoic seawater, *Chem. Geol.*, *161*(1–3), 59–88, doi:10.1016/S0009-2541(99)00081-9.

Vetter, L., R. Kozdon, C. I. Mora, S. M. Eggins, J. W. Valley, B. Hönisch, and H. J. Spero (2013), Micron-scale intrashell oxygen isotope variation in cultured planktic foraminifers, *Geochim. Cosmochim. Acta*, *107*, 267–278, doi:10.1016/j.gca.2012.12.046.

Weiner, S., and J. Erez (1984), Organic matrix of the shell of the foraminifer, Heterostegina depressa, *J. Foraminiferal Res.*, *14*(3), 206–212, doi:10.2113/gsjfr.14.3.206.

York, D. (1968), Least squares fitting of a straight line with correlated errors, *Earth Planet. Sci. Lett.*, *5*, 320–324, doi:10.1016/S0012-821X(68)80059-7.

Zachos, J. C., M. Pagani, L. Sloan, E. Thomas, and K. Billups (2001), Trends, rhythms, and aberrations in global climate 65 Ma to present, *Science*, *292*(5517), 686–693, doi:10.1126/science.1059412.